in: Saratov Fall Meeting 2004: Optical Technologies in Biophysics and Medicine VI,
Edited by V V Tuchin, Proc. SPIE 5771: 74-86 (2005)
(ISBN: 08194-57523) // Invited

Low and high orders light scattering within the dispersible media

E. Berrocal[*], V.P. Romanov[**], D.Y. Churmakov[*] and I.V. Meglinski[*]
[*] – School of Engineering, Cranfield University, Cranfield, MK43 0AL, UK
[**] – Physics Department, St. Petersburg State University, 198504 Petrodvoretz, Russia

ABSTRACT

Sprays, aerosols as well as other industrially relevant turbid media can be characterized by light scattering techniques. However these techniques often fall into the intermediate scattering regime where the average number of times a photon is scattered is too great for single scattering to be assumed, but too few for the diffusion approximation to be applied. We present the results of theoretical study provided details of scattering of laser radiation in the intermediate single-to-multiple scattering regime. Crossed fiber optic source-detector geometry is considered to separate the intensity of single scattering from higher scattering orders. A quantitative analysis of scattering orders in the intermediate single-to-multiple scattering regime is presented. Agreement between the analytical and Monte Carlo techniques both used for the calculation of double light scattering intensity is demonstrated. Influence of detector numerical aperture on the scattering orders is shown for the intermediate single-to-multiple scattering regime. The method used can be applied to verify analytical results indirectly against experiment via Monte Carlo calculations that include the imperfections of the experiment.

Keywords: spray diagnostics, transition single-to-multiple scattering, intermediate regime, scattering order

1. INTRODUCTION

The scattering of light by disperse randomly inhomogeneous scattering media is important in many applications including optical diagnostics in meteorology, powder industries and sprays for combustors, firefighting, drug and agrochemical delivery, and biomedicine. In all these applications knowledge/measurements of optical parameters of disperse medium is required. Typical parameters measured are the mean free transport path-length, shape and size of the scattering particles and their density within the medium. If the scattering power of the medium is low (mean number of scattering events ≤ 3) these parameters can be recovered from the intensity of single scattered radiation, by assuming only single scattering takes place[1-3]. However, if the medium is turbid (mean number of scattering events > 6) the intensity due to high orders of scattering dominates that due to single scattering at the detector, and the single scattering assumption becomes invalid. Nevertheless, the average parameters of such medium can be obtained by the diffusion approximation[4,5].

Greater complications arise in the intermediate case (mean number of scattering events ~ 3-6), where the average number of scattering events is too high for single scattering to be assumed, but too low for the diffusion approximation to be applied. This situation is typical for many practical applications, including industrial sprays. It should be pointed out however, that in the field of sprays most currently available optical diagnostic instruments operate in media of low scattering power, using the single scattering assumption. The development of the instruments operating in the intermediate scattering regime is needed. The intermediate scattering regime is encountered when making measurements near the nozzle (as required for boundary condition data for computational fluid dynamics (CFD) calculations of spray systems, or to validate liquid breakup models), or when the path length of the light in the spray is long (as in the case of high flow rate mixing systems such as fuel atomizers for large combustors). To develop such instruments, and to characterize their accuracy numerical technique predicting optimal parameters of the detector, signal-to-noise, sampling volume, *etc*. is highly required.

For dilute intermediate scattering media the parameters of scattering particles can be obtained from the angular dependence of the scattered light intensity, from attenuation of light due scattering and absorption, or

Correspondence: E-mail: i.meglinski@cranfield.ac.uk; Fax: +44 1234 750425

In the intermediate scattering regime both single and high order terms of the series should be considered. To separate these scattering terms from each other we apply an idea originally suggested in the study of critical phenomena and second order phase transition[27]. Schematically this idea is represented in Fig.2.

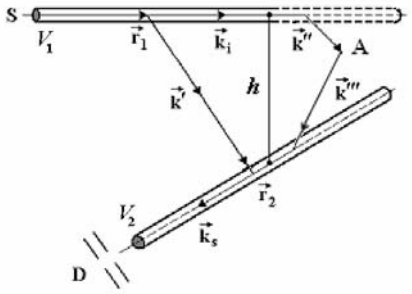


Fig.2. Schematic illustrating the experimental/computational geometry used to account for single-to-higher orders laser scattering. The laser source ***S*** and detector ***D*** sample two cylindrical volumes, within which single scattering occurs at the points $\vec{r}_1$ and $\vec{r}_2$. If the volumes are separated by distance *h*, the detector collects only double and higher orders of scattering. $\vec{k}_i$, $\vec{k}'$ and $\vec{k}_s$ are the wave-vectors of the incident, intermediate and detected double-scattered light, respectively. $\vec{k}''$ and $\vec{k}'''$ the are intermediate wave vectors for triple light scattering, ***A*** is a point of integration over the all scattering volume.

The laser source ***S*** illuminates the medium with a thin cylindrical laser beam. Detector ***D*** is confined by series of small aperture diaphragms, so that detected radiation is localized in a cylindrical volume V_2, which is equal to the volume filled by incident laser beam V_1 (see Fig.2). Thus, if V_1 and V_2 do not intersect, photons must experience at least two scattering events in order to be detected. Similarly, for singly scattered photons to reach the detector, the volumes must intersect i.e. *h* must be less than the diameter of cylinder (see Fig.2). When the characteristic diameter of the scattering volume *V* is much less than the distance to the observation point, the intensity of single scattering light takes the form[5,26,27]:

$$I_{(1)} = \frac{I_0 V}{r^2}\frac{k_0^4}{(4\pi)^2}\left(\delta_{\alpha\beta} - \frac{k_{s\alpha}k_{s\beta}}{k^2}\right)^2 G(\vec{q})e^{-\mu_t(l_1+l_2)}. \qquad (1)$$

Here, I_0 is the intensity of the incident light, *V* is the scattering volume, *r* is the distance to the observation point, $k_0=\omega/c$, ω is the cycle frequency, *c* is the speed of light in vacuum, α and β are the indices of polarization of the incident and scattered light, respectively. $G(\vec{q})$ is the correlation function of the permittivity fluctuations. The exponential multiplier describes attenuation along a path l_1 before and a path l_2 after the scattering. μ_t is the extinction coefficient, describing the attenuation of light due to elastic and inelastic interactions of laser radiation within the medium: $\mu_t = \mu_s + \mu_a$, where μ_s and μ_a are the scattering and absorption coefficients, respectively, $\vec{q} = \vec{k}_s - \vec{k}_i$ is the scattering wave vector. Vectors $\vec{k}_s$ and $\vec{k}_i$ are the wave-vectors of the incident and scattered light, respectively, and $\vec{k}$ can be expressed as a vector $k\frac{\vec{r}}{r}$, where $\frac{\vec{r}}{r}$ is the direction towards an observation point. A factor $\left(\delta_{\alpha\beta} - \frac{k_{s\alpha}k_{s\beta}}{k^2}\right)^2$ accounts for the transverse nature of the scattered electromagnetic wave.

The intensity of double scattering is given by:

$$I_{(2)} = \frac{I_0 k_0^8}{r^2 (4\pi)^4} \int_{V_1} d\vec{r}_1 \int_{V_2} d\vec{r}_2 \, F_{\alpha\beta}(\vec{k}_s, \vec{k}_i, \vec{k}') \frac{1}{\left|\vec{r}_2 - \vec{r}_1\right|^2} G(\vec{k}' - \vec{k}_i) G(\vec{k}_s - \vec{k}') \exp\left[-\mu_t (l_1 + l_2 + \left|\vec{r}_2 - \vec{r}_1\right|)\right], \quad (2)$$

where

$$F_{\alpha\beta}(\vec{k}_s, \vec{k}_i, \vec{k}') = \left(\delta_{\alpha\eta} - \frac{k'_\alpha k'_\eta}{k^2}\right)\left(\delta_{\alpha\nu} - \frac{k'_\alpha k'_\nu}{k^2}\right)\left(\delta_{\beta\eta} - \frac{k_{s\beta} k_{s\eta}}{k^2}\right)\left(\delta_{\beta\nu} - \frac{k_{s\beta} k_{s\nu}}{k^2}\right) \quad (3)$$

is the polarization factor, V_1 is the illuminated volume, the scattered light is collected by the detector from the volume V_2. Summation occurs over the indices (except over α and β) where a quantity has more than one index. Equation (2) describes the intensity of doubly scattered light reaching the detector i.e. singly scattered light entering volume V_2 and being scattered into the $\vec{k}_s$ direction with a wave-vector $\vec{k}_s - \vec{k}'$. Note, all first order scattering events occur in the volume V_1 with a wave-vector $\vec{k}' - \vec{k}_i$, where $\vec{k}'$ is the intermediate wave-vector (see Fig.2).

If $\vec{k}_i$ and $\vec{k}_s$ lie in the XZ plane, i.e. $k_{iy} = k_{sy} = 0$, and polarization vectors ($\vec{e}_\alpha = \vec{e}_i = \vec{e}_\beta = \vec{e}_s = \vec{e}_y$) then in single scattering $\left(\delta_{\alpha\beta} - \frac{k_{s\alpha} k_{s\beta}}{k^2}\right)^2 = 1$ and the double scattering polarization factor becomes

$$F_{\alpha\beta}(\vec{k}_s, \vec{k}_i, \vec{k}') = \left(1 - \frac{k_y'^2}{k^2}\right)^2. \quad (4)$$

If $\vec{e}_i = \vec{e}_y$, whereas $\vec{e}_s$ lay in (XZ) plane, then the polarization factor $\left(\delta_{\alpha\beta} - \frac{k_{s\alpha} k_{s\beta}}{k^2}\right)^2$ is equal to zero. In this case the depolarized single light scattering intensity is equal to zero as well, whereas the depolarized component of the double scattering is not equal to zero due to:

$$F_{\alpha\beta}(\vec{k}_s, \vec{k}_i, \vec{k}') = \frac{k_y'^2}{k^2}\left(1 - \frac{k_y'^2}{k^2} - \frac{(\vec{k}_s \vec{k}')^2}{k^4}\right) = \frac{k_y'^2}{k^2}\left\{\left(\frac{k'_z}{k} - \frac{k_{sz}(\vec{k}_s \vec{k}')^2}{k^3}\right)^2 + \left(\frac{k'_x}{k} - \frac{k_{sx}(\vec{k}_s \vec{k}')^2}{k^3}\right)^2\right\} \neq 0. \quad (5)$$

Here we take into account that $k_{sx}^2 + k_{sz}^2 = k^2$, as $k_{sy} = 0$. Thus, when the contribution of high order scattering is negligible and double scattering dominates, its depolarized component can be measured separately.

The comparison of the single and double light scatterings permits us to extract information on the scattering media. To illustrate this, let us consider a weakly scattering medium of spherical scattering particles with the correlation function $G(q)$ described by the Rayleigh-Gans approximate formula:

$$G(q) = N\left(\frac{4\pi\Delta\varepsilon}{q^3}\left[\sin(qa) - qa\cos(qa)\right]^2\right)^2, \quad (6)$$

where N is the particle density number, $\Delta\varepsilon$ is the difference of permittivities of particles and host medium, d is a particle diameter.

If the diameter of particles is less than the wavelength of incident radiation, $G(q)$ can be described as:

$$G(q) \approx \left(\frac{2\pi\Delta\varepsilon}{3}\right)^2 a^6 N. \quad (7)$$

Hence, the intensities of single and double light scatterings are:

$$I_{(1)} = \frac{I_0 V}{r^2} k_0^4 \left(\frac{\Delta\varepsilon}{6}\right)^2 a^6 N\,, \tag{8}$$

and

$$I_{(2)} = \frac{I_0 k_0^8}{r^2}\left(\frac{\Delta\varepsilon}{6}\right)^4 \int_{V_1} d\vec{r}_1 \int_{V_2} d\vec{r}_2 \; \frac{1}{|\vec{r}_2 - \vec{r}_1|^2} \frac{k_y'^2}{k^2}\left(1 - \frac{k_y'^2}{k^2} - \frac{(\vec{k}_s \vec{k}')^2}{k^4}\right) a^{12} N^2 \exp\left[-\mu_t (l_1 + l_2 + |\vec{r}_2 - \vec{r}_1|)\right], \tag{9}$$

respectively. It is easy to see that the ratio of $I_{(2)}$ and $I_{(1)}$ depends on the factor $(\Delta\varepsilon)^2 a^6 N$ describing optical properties of the medium. Thus the ratio of measured $I_{(2)}$ and $I_{(1)}$ gives the values of the medium optical parameters. However, to make the results obtained more reliable, higher orders of scattering should be taken into account. The evaluation of analytical expressions for the high scattering orders $I_{(3)}$, $I_{(4)}$, $I_{(5)}$, *etc.* is an extraordinary complex mathematical problem requiring the calculation of multi-fold integrals. The double scattering intensity calculation needs cumbersome computation of the six-fold integral (10), whereas $I_{(3)}$ requires calculation of nine-fold integral, $I_{(4)}$ twelve-fold integral, *etc*.

$$I_{(2)} = A \int_{-L_1/2}^{L_1/2} dl_1 \int_{-L_2/2}^{L_2/2} dl_2 \int_0^{R_1} r_1 dr_1 \int_0^{R_2} r_2 dr_2 \int_0^{2\pi} d\phi_1 \int_0^{2\pi} d\phi_2 \; \frac{1}{|\vec{R}_2 - \vec{R}_1|^2} \exp\left[-\mu_t (l_1 + l_2 + |\vec{R}_2 - \vec{R}_1|)\right], \tag{10}$$

where A is a constant, L_1 and L_2 are the cylinder lengths,

$$\begin{aligned} \vec{R}_1 &= \left(r_1 \cos\varphi_1, r_1 \sin\varphi_1, l_1\right) \\ \vec{R}_2 &= \left(l_2, h + r_2 \cos\varphi_2, r_2 \sin\varphi_2\right) \end{aligned}. \tag{11}$$

To avoid this complex calculation, the numerical MC technique can be applied to calculate the high order scattering terms.

3. MONTE CARLO METHOD

The exact implementation of the MC technique for calculation of scattering light intensity in an inhomogeneous scattering medium depends on the application[16-18,24,28]. The MC scheme presented here is suitable for the geometry described in Fig.2 and possesses the following characteristics. Incident radiation is considered normal to the surface of a scattering cube of 50 *mm*, defined in a 3D coordinate system (Fig. 3).

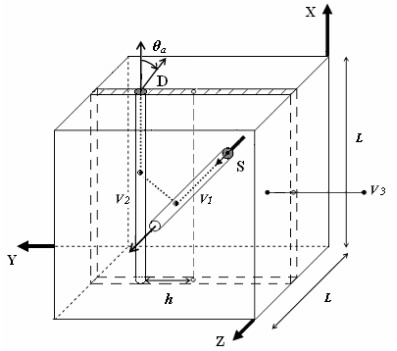


Fig.3. The scattering volume is a cube of L=50 *mm* defined in a 3D coordinate system. One of the corners of the cube corresponds to the origin of the (XYZ) frame.

The medium is assumed non-absorbing ($\mu_a = 0$), and homogeneous. The scattering coefficient μ_s is equal to 0.04 mm^{-1} and corresponds to an average propagation distance of $\langle l \rangle$ equaled to 25 *mm* (i.e. single scattering is largely dominated). The source ***S*** is defined by a flat laser beam of 1 *mm* diameter, which enters through the middle of the *XY* face of the sampling cube. This light source illuminates a cylindrical volume V_1 through

the scattering medium. The detector ***D*** is characterized by an aperture of 1 *mm* diameter located on the top of the cube and positioned at different distances *h* from the central axis of the cube.

MC modeling of the photon trajectories within the medium consists of following steps. The path-length of a photon packet between two scattering events is given by[12]:

$$l_i = -\frac{\ln(\xi)}{\mu_s}, \tag{12}$$

where ξ is a random number uniformly distributed between 0 and 1. To specify the position a photon and its direction of propagation, the absolute and local coordinate systems given in Figure 4 are used. After scattering the new direction is specified by the polar and azimuth angles, i.e. by θ_s and φ, respectively (see Fig.4).

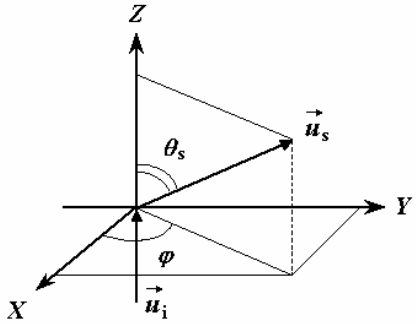


Fig.4. Cartesian coordinate system used to specify a position of a photon packet. Vectors $\vec{u}_i$ and $\vec{u}_s$ determine incident and scattered directions, respectively. In the local coordinate system, a new direction is given by the polar scattering angle θ_s and azimuth angle φ. The particular case where the absolute and local coordinate systems overlap is shown.

The directions of the photon packet propagation before and after the scattering are defined by unit vectors $\vec{u}_i$ and $\vec{u}_s$, vectors $\vec{u}_i$ and $\vec{u}_s$ being collinear to vectors $\vec{k}_i$ and $\vec{k}_s$, respectively. The following transformation relates them:

$$\begin{pmatrix} u_{sx} \\ u_{sy} \\ u_{sz} \end{pmatrix} = \begin{bmatrix} \frac{1}{\sqrt{1-u_{iz}^2}} u_{ix}u_{iz} & -\frac{1}{\sqrt{1-u_{iz}^2}} u_{iy} & u_{ix} \\ \frac{1}{\sqrt{1-u_{iz}^2}} u_{iy}u_{iz} & \frac{1}{\sqrt{1-u_{iz}^2}} u_{ix} & u_{iy} \\ -\sqrt{1-u_{iz}^2} & 0 & u_{iz} \end{bmatrix} \begin{pmatrix} \sin\theta_s \cos\varphi \\ \sin\theta_s \sin\varphi \\ \cos\theta_s \end{pmatrix}. \tag{13}$$

The direction of the photon packet $\vec{u}_i$ together with its free path length l_i determine the point at which the next scattering event takes place: $\vec{r}_{i+1} = \vec{r}_i + l_i\vec{u}_i$. At this point a new direction and path length are determined and the steps describes above are repeated again.

The polar scattering angle is sampled from a scattering phase function[21]:

$$p(\vec{k}_i, \vec{k}_s) = \frac{\sigma(\vec{k}_i, \vec{k}_s)}{\int_{4\pi} \sigma(\vec{k}_i, \vec{k}_s) \mathrm{d}\Omega_s}. \tag{14}$$

Depending on the purpose of the study, the Mie[1,2,30], Rayleigh-Gans[1,2] or Henyey-Greenstein[29] phase function is typically used. The change in polar angle θ_s is determined from its inverse cumulative probability density function (*iCPDF*)[31], $\theta_s = CPDF^{-1}(\xi)$. When the analytical form of the *iCPDF* is not available, *CPDF* is stored

in a lookup table[31,32] and the inverse transformation is performed before every scattering event. However, in this paper scattering has been restricted to the case of isotropic scattering to minimize the number of parameters. In this case θ_s is sampled from $\cos(\theta_s) = (2\xi - 1)$, and the change in the azimuthal angle φ is obtained from $\varphi = 2\pi\xi$.

Photon packets are assumed to have been detected if they reach the detector ***D*** with an incident angle θ_s which is less then detectors acceptance angle θ_a ($\theta_s \le \theta_a$). For each detected photon packet the scattering order and the distance h from the incident beam is stored in the data file. The intensity of different scattering orders is then determined by the number of photons recorded and can be plotted as a function of h. Due to the peculiarities of source-detector geometry, domination of single scattering and narrow numerical aperture (minimal $\theta_a = 2°$) a great number of photons are tracked. For this simulation, 10 billion photons have been calculated. This corresponds to 20 hours of computational time with a 2.5 *GHz* processor. It should be pointed out also that if the detectors acceptance angle is very small ($\theta_a < 2°$), the number of photon packets detected is very low, and consequently noisy, with the MC scheme described above. To obtain less noisy results for this angle ($\theta_a \sim 0°$) we use slightly different MC scheme[17,33]. This scheme uses the probability W that a photon packet scattered at the normal incidence to the detector:

$$W = p\left(\vec{k}_d - \vec{k}'\right) d\Omega_d e^{-\mu_t d} . \tag{15}$$

Here, $\vec{k}_d$ is the vector of normal towards the detector, $d\Omega_d$ is the elementary solid angle spanning a line normal to the detector and d is the distance between the photon scattering and detector. $p\left(\vec{k}_d - \vec{k}'\right)$ is the scattering phase function, constant for isotropic scattering: $p\left(\vec{k}_d - \vec{k}'\right) = 1/4\pi$. The intensity of scattering orders is obtained then by calculation of this probability for all the scattering events. This treatment significantly reduces the computational time (by a factor of ~ 100).

4. RESULTS AND DISCUSSIOS

In order to validate MC technique we compare the results of analytical calculations and numerical simulation for double light scattering intensity in frame of the source-detector geometry represented in Fig.2. For the analytical calculation of the double scattering intensity (10) we introduce the cylindrical coordinate frames (l_1, r_1, φ_1) and (l_2, r_2, φ_2). For the large distances h, i.e. $h >> R_1$, R_2, Eq.(10) is significantly simplified and for $\theta = \pi/2$, $I_{(2)}$ can be written as:

$$I_{(2)}(h) = A\pi^2 R_1^2 R_2^2 \int_{-L_1/2}^{L_1/2} dx \int_{-L_2/2}^{L_2/2} dz \frac{1}{x^2 + z^2 + h^2} \exp\left[-\mu_t \left(L + z - x + \sqrt{x^2 + z^2 + h^2}\right)\right]. \tag{16}$$

Here, $L+z-x = l_1+l_2$; R_1 and R_2 are the radii of V_1 and V_2 cylinders directed along the axes Z and X, respectively.

The results of simulation and analytical calculation of $I_{(2)}(h)$ are presented in Fig.5. The parameters of the cylinders are $L = L_1 = L_2 = 50$ *mm*, $R = R_1 = R_2 = 0.5$ *mm*. The finite volume of the scattering medium ($\mu_s = 0.04$ mm^{-1}) modelled is a cube of side 50 *mm*. The results of analytical calculation from equation 16 are shown by the dashed line. The circles represent the results of the MC simulation (see Fig.5-a). Both results agree well with the results of calculation by Eq.(10) shown by solid line (see Fig.5-a). Similar results are obtained for higher scattering ($\mu_s = 0.16$ mm^{-1}) of the medium (see Fig.5-b). With the geometry used here (see Fig.3) the intensity of the detected light is decreased by a factor of 400 by this increase in attenuation. The minimum distance s traversed by the photons from source (***S***) to detector (***D***) is ~ 40 *mm*. Good agreement between the results of calculation by Eqs.(10) and (16), and MC simulation for all $h > 2$ *mm* is obtained as well (see Fig.5-b).

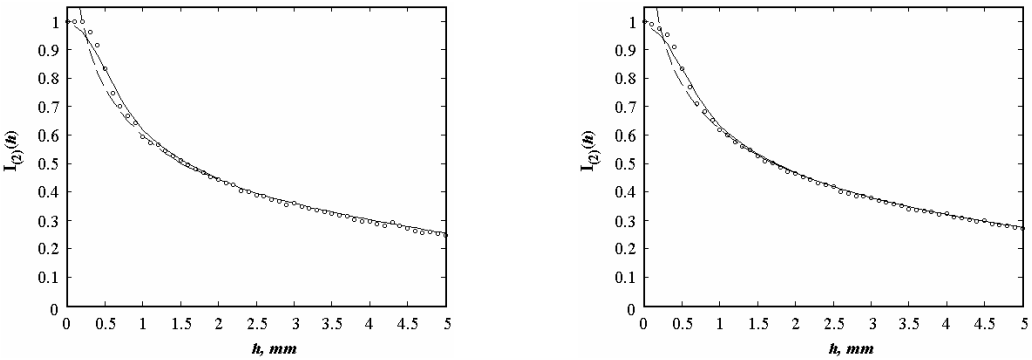


Fig.5. Intensity of the double light scattering in respect with the distance h between V_1 and V_2: a) $\mu_s = 0.04\ mm^{-1}$, b) $\mu_s = 0.16\ mm^{-1}$. The solid line represents the results of calculation by Eq.(10), dotted line is the results calculated by the approximate Eq.(16), circles are the results of MC simulation.

Equation 16 reduces to $I_{(2)}(h) \sim |\ln(h)|$ for $h \to 0$, i.e. it predicts the intensity of scattering goes to infinity, which is unphysical. The discrepancy between the exact Eq.(10), and approximate Eq.(16), formulas begins at $h = 1.2$ mm which is close to the diameter of cylinders. Analytical expressions for the high scattering orders (i.e. $I_{(3)}$, $I_{(4)}$ etc.) differ from the expressions for $I_{(1)}$, $I_{(2)}$ (see Eqs.(1)–(2)), and involve multi-order integrals. This is due to presence of intermediate integration over the total scattering volume as schematically shown for $I_{(3)}$ in Fig.2. However, using the MC technique it is possible to show that due to the presence of the intermediate integrations, these high-order integrals do not possess a logarithmic singularity as Eq.(16), i.e. they are the smooth functions for small h [34].

The 3, 4, 5 and 10-th scattering orders are calculated by the MC technique for the scattering medium with $\mu_s = 0.04\ mm^{-1}$ (Fig.6).

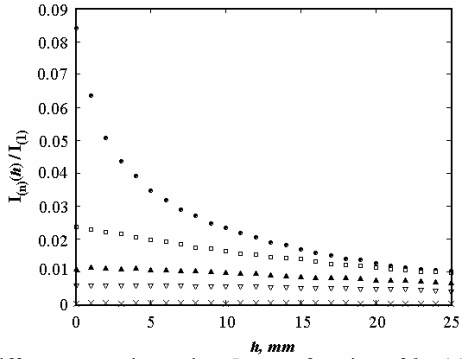


Fig.6. Normalized intensity of different scattering orders $I_{(n)}$ as a function of h : (•)˜ double scattering $I_{(2)}$, (□)˜ triple scattering $I_{(3)}$,(▲)˜ fourth order scattering $I_{(4)}$,(∇)˜ fifth order scattering $I_{(5)}$ and (x)˜ tenth order scattering $I_{(10)}$. The intensity of each scattering order is normalized to the intensity of single scattering $I_{(1)}$ at the $h = 0$.

The dependence of $I_{(2)}$ as a function of h is also included for comparison (see Fig.6). All the calculated intensities are normalized to the value of the single light scattering intensity $I_{(1)}$ at the $h = 0$. It is well seen that, as discussed above, $I_{(n),n \geq 3}$ are smooth functions of h separated from each other. The magnitude of the scattering orders of the series is ranged as: $I_{(3)}$ falls by a factor of 2.5 when h varies from 0 to 25 mm, $I_{(4)}$ decreases by 1.4, $I_{(5)}$ decreases by 1.1, and $I_{(10)}$ is effectively equal to zero (see Fig.6). For comparison $I_{(2)}$ is reduced by a factor of 9 in the same interval.

Figure 7 illustrates a ratio of n-th orders of scattering to single scattering intensity at the $h = 0$, i.e. $I_{(n)}(0)/I_{(1)}(0)$, where $n = \{3 \div 5, 10\}$. This ratio is monotonically increased with the increasing of the scattering

order. In the interval $\mu_s \sim 0.14–0.15\ mm^{-1}$ the values of $I_{(n)}/I_{(1)}$ becomes very close, and for higher μ_s an inversion of scattering orders takes place (see Fig.7). It is clear that the contribution of high scattering orders is significant, about 15–20% of the single scattering intensity at the $h = 0$ (see Fig.7) when $\mu_s \sim 0.1 \div 0.15\ mm^{-1}$. This interval illustrates the transition from single-to-multiple scattering regime, where the light transport can be described by the diffusion approximation. The obtained results are well agreed with the experimental results reported in Ref.35.

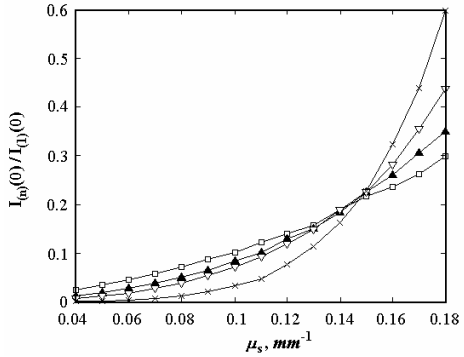


Fig.7. Normalized intensities of n-th scattering orders and single scattering intensity at $h = 0$, $I_{(n)}(0)/I_{(1)}$ as a function of scattering coefficient μ_s: triple scattering $I_{(3)}$ (□), fourth order scattering $I_{(4)}$ (▲), fifth order scattering $I_{(5)}$ (∇) and tenth order scattering $I_{(10)}$ (x).

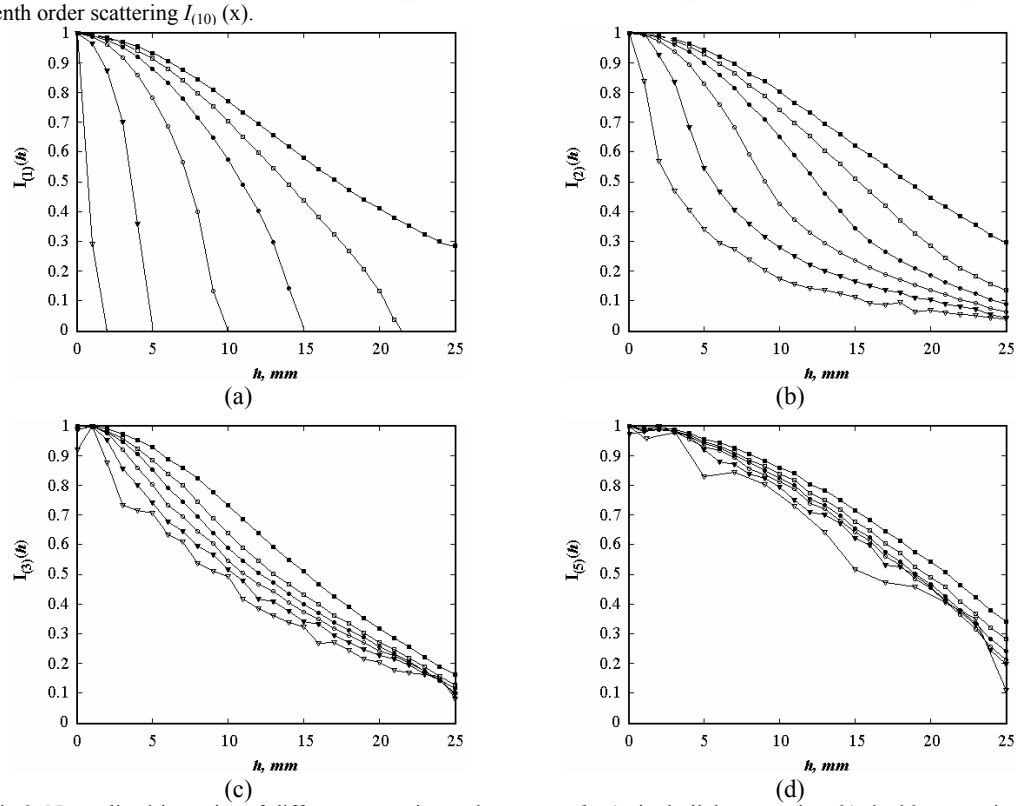


Fig.8. Normalized intensity of different scattering orders versus h: a) single light scattering; b) double scattering; c) triple scattering; d) fifth order scattering. The symbols represents different values of the detector numerical aperture: (∇) – 2°, (▼) – 10°, (○) – 20°, (●) – 40°, (□) – 60°, (■) – 90°.

Figures 8 and 9 present the results of a study of the detection parameters. The intensity of different scattering orders versus numerical aperture is shown in Fig. 8. It is seen that the dependence is more pronounced for single and double light scatterings (see Fig. 8-a and b). The high scattering orders (e.g. third and fifth) are independent to the detecting angle θ_a (see Fig. 8-c and d). This is explained by the fact that, the localization of mean path-length of the photon packets between source and detector is more critical for single and double scattering, and less for the high orders of scattering.

A quantitative fraction of these scattering orders as a function of numerical aperture is shown in Fig.9 for h = 0. Single scattering dominates at small θ_a ($\theta_a < 20°$), the contribution of the other scattering orders being relatively low. The contribution of the different scattering orders relative to the intensity of single scattering in this range of θ_a is shown in Fig. 10.

The sum of the intensities of high orders of scattering is represented by dashed line (see Fig.9). Note that the contribution of single and of multiple scattering becomes equal at a detector acceptance angle ≈ 20° ($\theta_a \approx$ 20°). As assumed, the contribution of single scattering decreases with increasing detector aperture, and from 20° multiple scattering dominates the detected signal ($0° < \theta_a < 90°$). This is logical, as with increasing θ_a the detector collects light scattered from an increasing volume of the medium.

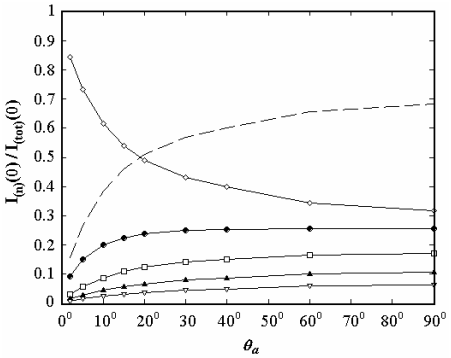


Fig.9. Results of MC calculation of the different scattering order intensities $I_{(n)}/I_{(tot)}$ versus angle detector aperture: (◊) – single scattering $I_{(1)}$, (•) – double scattering $I_{(2)}$, (□) – triple scattering $I_{(3)}$, (▲) – fourth order scattering $I_{(4)}$, (▽) – fifth order scattering $I_{(5)}$. The dashed line represents the relative contribution of multiple scattering to the total intensity, $(I_{(tot)}-I_{(1)})/I_{(tot)}$.

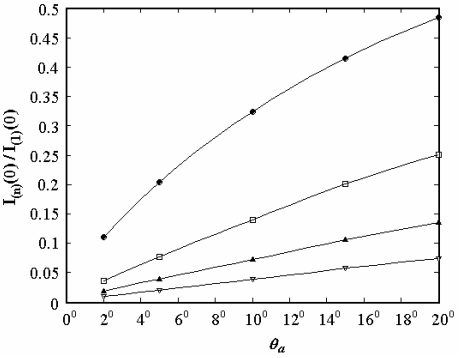


Fig.10. Normalized intensities of different scattering orders $I_{(n)}/I_{(1)}$ as a function of numerical aperture: (•) – double scattering, (□) – triple scattering, (▲) – fourth order scattering, (▽) – fifth order scattering.

5. SUMMARY AND CONCLUSIONS

An analysis of different scattering orders in the intermediate scattering regime has been carried out for a randomly inhomogeneous scattering medium with crossed source-detector geometry. The results

demonstrate good agreement between analytical and MC techniques. The influence of detector numerical aperture on the intensity of the different scattering orders is shown quantitatively. Particular attention is paid to the difficult intermediate regime, where the scattering power of the medium is too high for single scattering to be assumed but is too low for the diffusion approximation to be applied. The results show the characteristics of the transition from single to multiple scattering. The agreement between analytical and MC results validates the use of the MC approach in the intermediate scattering regime. The method used can be applied to verify analytical results against experiment indirectly via MC calculations that account for imperfections of the experiment, which are difficult to represent analytically.

The geometry chosen for the optical experiment is interesting in that it allows the experimenter to measure the intensity of single and higher scattering orders separately. It is possible to extract information on the absolute values of the medium optical properties from the ratio of single to higher scattering orders. The total intensity of the scattered light $I_{(tot)}(h)$ can be considered then as:

$$I_{(tot)}(h) = I_{(1)}(r_0) + I_{(p)}(h) = I_{(1)}(r_0) + I_{(2)}(h)\frac{(1-\gamma^n)}{1-\gamma},$$

where $r_0 \in V_{single}$, where V_{single} is an effective volume of single light scattering; $I_p(h) = \sum_{n\geq 2} I_{(n)}(h) = I_{(2)} + \gamma I_{(2)} + \gamma^2 I_{(2)} + \ldots + \gamma^{(n-1)} I_{(2)},\ \forall \gamma < 1,\ \gamma \approx \frac{I_{(2)}}{I_{(3)}} \approx \frac{I_{(3)}}{I_{(4)}} \approx \frac{I_{(4)}}{I_{(5)}} \approx \ldots \approx \frac{I_{(n-1)}}{I_{(n)}}$.

The MC simulations allow us to develop an iterative procedure to determine the contributions of the higher scattering orders (triple, quadruple *etc*. scattering) to the total intensity separately, thus, completing the task of experimental data processing. Both MC and analytical calculations show a strong logarithmic dependence of double light scattering from the distance h between illuminating and collecting volumes. Dependence of higher scattering orders is weaker and can be considered constant compare to the single order.

The MC method was successfully applied to calculate the intensities of different orders of scattering. These results can be used to infer the optical parameters of inhomogeneous media with the experimental geometry shown in Fig.2. The proposed experimental geometry (see Fig.2) can be used in a practical experiment to measure the particulate scattering field properties. Certainly, the illumination and detection volumes cannot be ideally cylindrical but with a laser of high confocal parameter and a tightly collimated detector they can be near cylindrical, and the MC code can be used to quantify the effect of these experimental imperfections. A further advantage of the suggested approach is that as well as the dependence of the scattered light intensity on the distance parameter h, the angular intensity dependence, i.e. the dependence on θ (see Eqs.10 and 16), can also be obtained.

This results in a greater amount of experimental information, $I_{(\mathrm{tot})}(\theta, h)$. In addition, the results support the use of the MC approach in the intermediate scattering regime, and provide details of transition from low scattering (when intensity of scattering orders drops with the scatters increasing) to high scattering (when increasing of intensity occurs in the range of scattering $0.08 \leq \mu_s \leq 0.1\ mm^{-1}$). The method used can be applied to verify the analytical results indirectly against experiment via MC calculations that include the imperfections of the experiment. For clarity we have considered the simplest case of spatially homogeneous scattering medium with an isotropic phase function. The procedure developed can readily be generalized for a case of anisotropic scatters, spatially inhomogeneous media and dispersed systems composed of particles of a different size. We intend to apply the MC code verified here to the estimation and suppression of errors in existing spray diagnostics and the development of new spray diagnostics.

ACKNOWLEDGEMENTS

The authors acknowledge the support of The Royal Society (Project no.: 15298), NATO (Project PST.CLG.979652), and the U.K. Overseas Research Scholarships.

REFERENCES

1. H.C. van de Hulst, Light scattering by small particles, Dover, N.Y., 1981.
2. C. Bohren, D. Huffman, Absorption and scattering of light by small particles, Wiley, N.Y., 1983.
3. A. Ishimaru, Wave propagation and scattering in random media, Oxford Univ. Press, Oxford, 1997.
4. B.A. van Tiggelen, S.E. Skipetrov, Wave scattering in complex media: from theory to applications, NATO Science series: II: Mathematics, Physics and Chemistry, Vol. 107, Kluwer Academic Publishers, 2003.
5. V.L. Kuz'min, V.P. Romanov, "Coherent phenomena in light scattering from disordered systems", Usp. Fiz. Nauk, 39(3), pp.231-260, 1996.
6. J.Q. Shen, U. Riebel, "Extinction by a large spherical particle located in a narrow Gaussian beam", Part. Part. Syst. Char. 18 (5-6), pp.254-261, 2001.
7. G. Gouesbet, B. Maheu, G. Grehan, "Light scattering from a sphere arbitrarily located in a gaussian beam, using a Bromwich formulation", J. Opt. Soc. Am. A. 5 (9), pp.1427-1443, 1988.
8. Z. Ma, H.G. Merkus, H.G. van der Veen, M. Wong, B. Scarlett, "On-line measurement of particle size and shape using laser diffraction", Part. Part. Syst. Char. 18 (5-6), pp.243-247, 2001.
9. M. Kocifaj, M. Drzik. "Retrieving the size distribution of microparticles by scanning the diffraction halo with a mobile ring-gap detector", J. Aerosol. Sci. 28 (5), pp.797-804, 1997.
10. F. Zhao, Z. Gong, H. Hu, M. Tanaka, T. Hayasaka, "Simultaneous determination of the aerosol complex index of refraction and size distribution from scattering measurements of polarized light", Appl. Opt. 36 (30), pp.7992-8001, 1997.
11. M.C. Jermy, D.A. Greenhalgh, "Planar dropsizing by elastic and fluorescence scattering in sprays too dense for phase Doppler measurement", Appl. Phys. B 71, pp.703-710, 2000.
12. I.M. Sobol', The Monte Carlo Method, The University of Chicago Press, Chicago, 1974.
13. G.I. Marchuk, G.A. Mikhailov, M.A. Nazaraliev, R.A. Darbinjan, B.A. Kargin, B.S. Elepov, The Monte Carlo method in atmospheric optics, Springer, Berlin, 1980.
14. V.P. Kandidov, "Monte Carlo methods in nonlinear statistical optics", Usp. Fiz. Nauk 39(12), pp.1243-1272, 1996.
15. M. Keijzer, S.L. Jacques, S.A. Prahl, A.J. Welch, "Light distributions in artery tissue: Monte Carlo simulations for finite-diameter laser beams", Laser Sur. Med. 9, pp.148-154, 1989.
16. I.V. Meglinsky, S.J. Matcher, "Modelling the sampling volume for skin blood oxygenation measurements," Med. Biol. Eng. Comput. 39(1), pp.44-50, 2001.
17. R.R. Meier, J.-S. Lee and D.E. Anderson, "Atmospheric scattering of middle UV radiation from an internal source", Appl. Opt. 17, pp.3216-3225, 1978.
18. C. Lavigne, A. Robin, V. Outters, S. Langlois, T. Girasole and C. Roze, "Comparison of iterative and Monte Carlo methods for calculation of the aureole about a point source in the Earth's atmosphere", Appl. Opt. 38(30), pp.6237-6246, 1999.
19. E.A. Bucher, "Computer Simulation of light pulse propagation for communication through thick clouds", Appl. Opt. 12, pp.2391-2400, 1973.
20. A.I. Carswell, "Laser measurements in clouds", in Clouds: their formation, optical properties and effects", A. Deepak, P.V. Hobbs, Eds., pp.363-406, Academic Press Inc., 1981.
21. G.E. Thomas, K. Stamnes, Radiative transfer in the atmosphere and ocean, Cambridge University Press, Cambridge, 1999.
22. M.C. Jermy, A. Allen, "Simulating the effects of multiple scattering on images of dense sprays and particle fields", Appl. Opt. 41(20), pp.4188-4196, 2002.
23. M.C. Jermy, A. Allen and A.K. Vuorenkoski, "Simulating the effect of multiple scattering on images of dense sprays", in: Optical and laser diagnostics, Proc. 1st Int. Conf." IOP Conference Series No.177, C. Arcoumanis and KTV Grattan, Eds., pp.89-94, 2003.
24. E. Berrocal, A. Allen and M. Jermy, "Monte Carlo simulation of laser imaging diagnostics in polydisperse dense sprays", in: Proc. SPIE, 2004 (in press).
25. S.M. Rytov, Yu.A. Kravtsov, V.I. Tatarski, Principles of statistical radiophysics, Springer, Berlin, 1987.
26. P.M. Chaikin, T.C. Lubensky, Principles of condensed matter physics, Cambridge University Press, Cambridge, 1995.
27. V.L. Kuzmin, V.P. Romanov, L.A. Zubkov, "Propagation and scattering of light in fluctuating media", Physics Reports 248(2-5), pp.71-368, 1994.

28. D.Y. Churmakov, I.V. Meglinski and D.A. Greenhalgh, “Influence of refractive index matching on the photon diffuse reflectance”, Phys. Med. Biol. 47(23), pp.4271-4285, 2002.
29. L. G. Henyey, J. L. Greenstein, “Diffuse radiation in the galaxy”, Astrophys. J. 93, pp.70-83, 1941.
30. G. Mie, “Considerations on the optic of turbid media, especially colloidal metal sols”, Ann. Physik 25, pp.377-442, 1908.
31. J. R. Zijp, J. ten Bosch, “Use of tabulated cumulative density functions to generate pseudorandom numbers obeying specific distributions for Monte Carlo simulations”, Appl. Opt. 33(3), pp.533-534, 1994.
32. D. Toublanc, “Henyey-Greenstein and Mie phase functions in Monte Carlo radiative transfer computations”, Appl. Opt. 35(18), pp.3270-3274, 1996.
33. E. Tilnet, S. Avrillier, M. Tualle, “Fast semianalytical Monte Carlo simulation for time-resolved light propagation in turbid media”, J. Opt. Soc. Am. A 13(9), pp.1903-1915, 1996.
34. L.V. Adzhemyan, L. Ts. Adzhemyan, L.A. Zubkov, V.P. Romanov, "Molecular light scattering of varying multiplicity", Sov. Phys. JEPT 53(2), p.278-281, 1981.
35. K.K. Bizheva, A.M. Siegel and D.A. Boas, “Path-length resolved dynamic light scattering in highly scattering random media: The transition to diffusing wave spectroscopy”, Phys. Rev. E 58, pp.7664-7667, 1998.



https://dspace.org/

Low and high orders light scattering within the dispersible media.

Berrocal, Edouard; Romanov, V. P.; Churmakov, D. Y.; Meglinski, I. V.

2005-06-01T00:00:00Z

http://dspace.lib.cranfield.ac.uk/handle/1826/978

Proceedings of SPIE Volume: 5771. Saratov Fall Meeting 2004: Optical Technologies in Biophysics and Medicine VI. E. Berrocal, V. P. Romanov, D. Y. Churmakov, I. V. Meglinski, Low and high orders of light scattering within the dispersible media. pp. 74-86

Downloaded from a DSpace repository. https://dspace.org/